Molecular Biology of the Cell
Vol. 17, 4014–4026, September 2006

BLOC-1 Complex Deficiency Alters the Targeting of Adaptor Protein Complex-3 Cargoes

G. Salazar,*† B. Craige,*†‡ M. L. Styers,*§ K. A. Newell-Litwa,*‡§ M. M. Doucette,*‖ B. H. Wainer,*¶ J. M. Falcon-Perez,# E. C. Dell'Angelica,# A. A. Peden,@ E. Werner,* and V. Faundez*‡**

*Department of Cell Biology, ‡Graduate Program in Biochemistry, Cell, and Developmental Biology, **Center for Neurodegenerative Disease, and ¶Department of Pathology and Laboratory Medicine, Emory University, Atlanta, GA 30322; ‖College of Health and Human Sciences, Georgia State University, Atlanta, GA 30302; #Department of Human Genetics, University of California, Los Angeles, CA 90095; and @Cambridge Institute for Medical Research, Cambridge CB2 2XY, United Kingdom

Submitted February 6, 2006; Revised May 16, 2006; Accepted May 31, 2006
Monitoring Editor: Sandra Lemmon

Mutational analyses have revealed many genes that are required for proper biogenesis of lysosomes and lysosome-related organelles. The proteins encoded by these genes assemble into five distinct complexes (AP-3, BLOC-1-3, and HOPS) that either sort membrane proteins or interact with SNAREs. Several of these seemingly distinct complexes cause similar phenotypic defects when they are rendered defective by mutation, but the underlying cellular mechanism is not understood. Here, we show that the BLOC-1 complex resides on microvesicles that also contain AP-3 subunits and membrane proteins that are known AP-3 cargoes. Mouse mutants that cause BLOC-1 or AP-3 deficiencies affected the targeting of LAMP1, phosphatidylinositol-4-kinase type II alpha, and VAMP7-TI. VAMP7-TI is an R-SNARE involved in vesicle fusion with late endosomes/lysosomes, and its cellular levels were selectively decreased in cells that were either AP-3- or BLOC-1–deficient. Furthermore, BLOC-1 deficiency selectively altered the subcellular distribution of VAMP7-TI cognate SNAREs. These results indicate that the BLOC-1 and AP-3 protein complexes affect the targeting of SNARE and non-SNARE AP-3 cargoes and suggest a function of the BLOC-1 complex in membrane protein sorting.

INTRODUCTION

Membrane enclosed organelles possess distinctive protein compositions maintained by vesicle formation and vesicle fusion mechanisms. Vesicles are formed by coat and coat accessory molecules that selectively regulate the concentration of specific membrane proteins into departing vesicles. Once formed, vesicle contents are delivered to target membranes by vesicle fusion. This process depends on the pairing of fusogenic membrane proteins generically known as R- or vesicle (v)-SNAREs and Q- or target (t)-SNAREs (Springer *et al.,* 1999; Bonifacino and Glick, 2004; Hong, 2005). Vesicle formation by coats and fusion by SNAREs is likely to be coordinately regulated, as suggested by the specific subcellular localizations that coats and SNAREs possess (Robinson, 2004; Hong, 2005). Predictably, coats either interact with and/or sort SNAREs. However, SNARE sorting mechanisms have been described only for a limited number of the SNAREs known to eukaryotic cells (Gurkan *et al.,* 2005). For example, COPII interacts/sorts the R-(v)-SNAREs Bos1p and Bet1p into vesicles (Matsuoka *et al.,* 1998; Springer and Schekman, 1998); the adaptors GGA1–2 sort the yeast Q-(t)-SNARE Pep12p (Black and Pelham, 2000); epsinR sorts/interacts with the Q-(t)-SNARE Vti1b (Hirst *et al.,* 2004); the adaptor complex AP-3 sorts or interacts with the R-(v)-SNAREs VAMP7-TI (Martinez-Arca *et al.,* 2003) and engineered variants of VAMP2 (Salem *et al.,* 1998); and the adaptor complex AP-1 sorts/interacts with VAMP4 (Peden *et al.,* 2001). These coat-SNARE interactions define prebudding interactions of the vesicle sorting and fusion machineries. However, it is poorly understood in vertebrates whether 1) these interactions persist at later stages once a vesicle is formed and cargo concentration is completed and 2) if molecules or complexes other than coats affect SNARE targeting. Noncomplementing mutant alleles in a vesicle transport pathway could provide valuable tools to explore these questions.

Genetic deficiencies in the biogenesis of lysosomes and lysosome-related organelles are collectively known in humans as Hermansky-Pudlak syndrome (OMIM 203300; Li *et al.,* 2004; Di Pietro and Dell'Angelica, 2005). Natural and engineered mutations in the mouse orthologues of Hermansky-Pudlak genes and their interactors trigger a syndrome in mice characterized by oculocutaneous pigment dilution, platelet disfunction (Li *et al.,* 2004; Di Pietro and Dell'Angelica, 2005), and in some cases neurological disorders (Kantheti *et al.,* 1998, 2003; Nakatsu *et al.,* 2004; Seong *et al.,* 2005). The majority of the 14 genes identified so far assemble into five major protein complexes: AP-3 (adaptor protein complex 3), BLOC-1-3 (biogenesis of lysosome-related organelle complex), and HOPS (homotypic vacuolar protein sorting or

This article was published online ahead of print in *MBC in Press* (http://www.molbiolcell.org/cgi/doi/10.1091/mbc.E06–02–0103) on June 7, 2006.

† These authors contributed equally to this work.

§ These authors contributed equally to this work.

Address correspondence to: Victor Faundez (faundez@cellbio.emory.edu).

VPS class C complex; Di Pietro and Dell'Angelica, 2005). Of these complexes, the adaptor complex AP-3 functions in early endosomes where it is involved in protein sorting and vesicle biogenesis (Faundez *et al.*, 1998; Peden *et al.*, 2004). Vesicles generated by AP-3 carry membrane proteins bound to lysosomes, lysosome-related organelles, and synaptic vesicles, as illustrated by the AP-3 deficiency phenotypes (Kantheti *et al.*, 1998; Feng *et al.*, 1999; Yang *et al.*, 2000; Kantheti *et al.*, 2003; Nakatsu *et al.*, 2004; Seong *et al.*, 2005) as well as the proteome of AP-3–generated microvesicles (Salazar *et al.*, 2005b). Although BLOC complexes and AP-3 are thought to participate in the same vesicle transport pathway, the function of the BLOC complexes is less well understood (Li *et al.*, 2004; Di Pietro and Dell'Angelica, 2005). A potential function of BLOC complexes is suggested by the interactions reported for BLOC individual subunits. In fact, two subunits of the BLOC-1 complex, pallidin and snapin, are capable of interacting with the endocytic SNAREs syntaxin 13 (Huang *et al.*, 1999; Moriyama and Bonifacino, 2002) and SNAP23-25 (Ilardi *et al.*, 1999; Ruder *et al.*, 2005; Tian *et al.*, 2005), respectively. Furthermore, down-regulation of another BLOC-1 subunit, dysbindin, decreases the levels of a subset of synaptic proteins including SNAP25 (Numakawa *et al.*, 2004). These observations suggest that BLOC-1 complexes may participate in the targeting of specific SNAREs (Li *et al.*, 2004; Di Pietro and Dell'Angelica, 2005). However, it is unknown whether BLOC-1 complexes could also participate in AP-3 adaptor–dependent membrane protein sorting. In this article, we explore this hypothesis and demonstrate that BLOC-1 and AP-3 protein complexes are present on the same organelles and affect the targeting of AP-3 cargoes and AP-3 interacting R-(v)-SNAREs.

MATERIALS AND METHODS

Antibodies

The following antibodies were used: mouse anti-synaptophysin SY38 (Chemicon, Temecula, CA), anti-β-actin (Sigma, St. Louis, MO); anti-γ- and anti-α-adaptins, anti-syntaxin 8, and anti-Vti1b (Signal Transduction Laboratories, Franklin Lakes, NJ); anti-transferrin receptor (H68.4, Zymed, South San Francisco, CA). Anti-SV2 (10H4), anti-delta (SA4), and anti-mouse Lamp1 (ID4B) were from the Developmental Studies Hybridoma Bank at the University of Iowa. Anti-VAMP2 (69.1) was purchased from Synaptic Systems (Göttingen, Germany). AP-3 polyclonal antibodies and affinity-purified ZnT3 antibodies have already been described (Faundez *et al.*, 1998; Salem *et al.*, 1998; Salazar *et al.*, 2004b). Mouse anti-β-3B adaptin was purchased from BD Transduction Laboratories (Lexington, KY). Mono-specific affinity-purified polyclonal antibodies against phosphatidylinositol-4-kinase type IIα were reported by Guo *et al.* (2003). Rabbit anti-syntaxin 2 was from Calbiochem (San Diego, CA). Mouse anti-VAMP7 (Advani *et al.*, 1999), rabbit anti syntaxin 7 (Prekeris *et al.*, 1999), and rabbit anti-syntaxin 13 were already described (Prekeris *et al.*, 1998). Rabbit anti-VAMP3 and anti-VAMP8 were from Abcam (Cambridge, MA). Rabbit anti-pallidin and -dysbindin were described (Starcevic and Dell'Angelica, 2004).

Cell Culture

PC12 ZnT3-HA clone 4 cells were cultured following established procedures (Salazar *et al.*, 2004b). Brefeldin A treatments were performed using 10 μg/ml brefeldin A according to Salazar *et al.* (2004a, 2004b, 2005b). *Pearl*, *pallid*, *cocoa*, *pale ear*, *mocha*, and wild-type skin fibroblasts were grown in DMEM medium (Cellgro, Herndon, VA; 4.5 g/l glucose) supplemented with 10% fetal calf serum (Hyclone, Logan, UT), 100 U/ml penicillin, and 100 μg/ml streptomycin.

Subcellular Fractionation and Vesicle Isolation

PC12 cell differential fractionation and glycerol sedimentation were performed in intracellular buffer (38 mM potassium aspartate, 38 mM potassium glutamate, 38 mM potassium gluconate, 20 mM MOPS-KOH, pH 7.2, 5 mM reduced glutathione, 5 mM sodium carbonate, 2.5 mM magnesium sulfate, 2 mM EGTA) according to Clift-O'Grady *et al.* (1998) and Salazar *et al.* (2004b). Brain microvesicle subcellular fractionation, velocity sedimentation in glycerol gradients, and microvesicle immunomagnetic isolations were performed using methods detailed previously (Salazar *et al.*, 2004a, 2004b, 2005b).

All gradient fractions were analyzed by immunoblot, and immunoreactivity was revealed by ECL. Immunoreactive bands were quantified using NIH Image 1.62 software as described (Salazar *et al.*, 2004b).

Microvesicle coating assays were performed as described using glycerol gradient-isolated PC12 VAMP2-N49A–radiolabeled vesicles (Faundez *et al.*, 1998).

Mass Spectrometry

AP-3 microvesicle preparation was described in Salazar *et al.* (2005b). Nano-HPLC-MS/MS analysis was performed at the Emory Microchemical Facility using a QSTAR XL (Applied Biosystems, Foster City, CA) hybrid quadrupole tandem mass spectrometer interfaced with an Ultimate nano-HPLC system (LC Packings, Sunnyvale, CA). The mass spectrometer was operated in positive-ion mode using information-dependent acquisition to acquire a single MS scan (m/z 400-1900 scan range) followed by up to two MS/MS scans (m/z 50–1900 scan range). A rolling collision energy was used for the MS/MS scans. The data were analyzed using the ProID (Applied Biosystems) and MASCOT (www.matrixscience.com) search algorithms. Criteria to identify positive hits in mass spectrometry were described (Salazar *et al.*, 2005b).

Microscopy

Cells were fixed and processed for immunofluorescence as described (Faundez *et al.*, 1997). Secondary antibodies used were Alexa-conjugated goat anti-mouse 488, goat anti-mouse 555, goat anti-rabbit 647 (Molecular Probes, Eugene, OR). All secondary antibodies were used at 1:1000 dilution. Images were acquired using either deconvolution or confocal microscopy. Deconvolution microscopy image acquisition was performed with a scientific-grade cooled charge-coupled device (Cool-Snap HQ with ORCA-ER chip) on a multiwavelength, wide-field, three-dimensional microscopy system (Intelligent Imaging Innovations, Denver, CO), based on a 200M inverted microscope using a 63× numerical aperture 1.4 lens (Carl Zeiss, Thornwood, NY). Fluorescently labeled samples were imaged at room temperature using a Sedat filter set (Chroma Technology, Rockingham, VT), in successive 0.20-μm focal planes. Out-of-focus light was removed with a constrained iterative deconvolution algorithm (Swedlow *et al.*, 1997). Confocal microscopy was performed in an Axiovert 100M microscope (Carl Zeiss) coupled to an Argon ion laser. Images were acquired with LSM 510 sp1 software (Carl Zeiss) using a Plan Apochromat 63×/1.4 oil DiC objective. Images were processed and analyzed using Metamorph software Version 3.0 (Universal Imaging, West Chester, PA). All images were thresholded to similar levels. Fluorescent signal colocalization or overlapping was determined as follows. For each cell, an optical section obtained through the nuclear equator was analyzed. Pixels containing both fluorescent signals were considered colocalized or overlapped. This value was expressed as a percent of the total number of pixels positive for just one fluorochrome. Data were obtained from at least two independent experiments and numbers in parentheses correspond to the total number of cell analyzed.

Immunoperoxidase staining on brain sections has been described in detail (Salazar *et al.*, 2004a). Immunocomplexes were detected by species-specific VECTASTAIN ABC kit (Vector Laboratories, Burlingame, CA) according to manufacturer's instructions.

Surface LAMP1 Determinations

Cells were fixed and stained in suspension as described above. Surface staining was determined by staining cells in the absence of detergent. Total levels were assessed by staining in the presence of 0.02% saponin (Styers *et al.*, 2004). Antibody fluorescence was analyzed using a FACscalibur System (BD Biosciences, Franklin Lakes, NJ). Results were obtained from three independent experiments. Three independent cell isolates of each genotype were analyzed per experiment. Fluorescence intensity determinations per independent cell isolate and per experiment were performed in at least duplicate, each one containing at least 10,000 cells. Results were analyzed using FloJo version 6.0 (Tree Star, Ashland, OR) to obtain the mean fluorescence intensity of the population. The mean fluorescence intensity of the C57B cell isolate 1 was arbitrarily defined as 100% to normalize the values of all other cell isolates and genotypes.

Biotinylation was performed as described (Salazar and Gonzalez, 2002).

Flow Cytometry Analysis of Cellular AP-3 Content

Fibroblasts were grown in 10-cm Petri dishes. Cell were washed with phosphate-buffered saline (PBS) and lifted off the plate with PBS 25 mM EDTA for 20 min at 4°C. Cell were sedimented at 36 × *g* for 5 min at 4°C. Cell pellets were resuspended in intracellular buffer or intracellular buffer (Clift-O'Grady *et al.*, 1998) plus 0.02% saponin (perforated) during 10 min at 4°C. A set of saponin-treated cells was further incubated with 0.5 M Tris, pH 8 (Perforated + Tris), for additional 10 min at 4°C to remove adaptors (Chang *et al.*, 1993). Cells were fixed in paraformaldehyde 4% during 10 min, centrifuged, and resuspended in fresh paraformaldehyde for 20 min. After two washes with PBS, samples were incubated with block (2% BSA, 1% fish skin gelatin 0.02% saponin, and 15% horse serum in PBS) for 30 min at RT and then with anti-delta antibody in block for 30 min at 37°C. Alexa 488–conjugated anti-

A

Protein	GI Number	Peptide	Peptide #	Round
DYSBINDIN	17390817	LLSVQQDFTSGLK	4	A
SNAPIN	13879528	VALDLDPYVK	1	A
		VVLVNNILQNAQER	1	A
MUTED	27684693	AEVDAEHRK	1	B
		LQAATDSIHR	2	B
		NMIQETNER	1	B
		MLQWEEFLR	3	B
PALLIDIN	34856819	SPDEGLIEDLALEDR	3	B
		ALQELTQNQVVLLDTLEQEISK	1	B

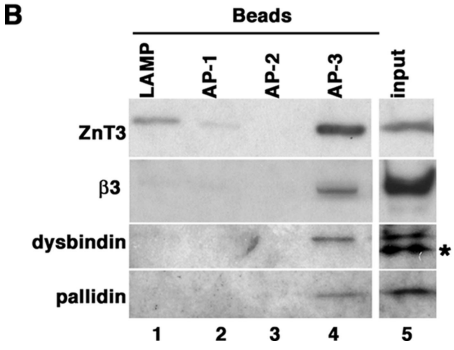

Figure 1. BLOC-1 subunits are present in neuroendocrine AP-3 microvesicles. (A) BLOC-1 subunit peptides identified by MS/MS. The number of times that a peptide was identified (peptide #) and the mass spectrometry round (A or B) are depicted. (B) Glycerol gradient purified PC12 microvesicles were bound to magnetic beads coated with either human specific LAMP1 (lane 1), AP-1 γ-subunit (lane 2), AP-2 α-subunit antibodies (lane 3), or AP-3 delta adaptin monoclonal antibodies (lane 4). Bead-bound vesicles were resolved by SDS-PAGE and analyzed by immunoblot with antibodies against ZnT3, AP-3 β3-adaptin, and the BLOC-1 subunits dysbindin and pallidin. Asterisk marks a nonspecific immunoreactive band observed in PC12 cells. Input represents 10% of the vesicles used per assay (n = 2).

mouse antibodies were used at 1:1000 dilution for 30 min at 37°C. AP-3 fluorescence intensity was determined using a FACscalibur System (BD Biosciences) in at least 10,000 cells. All determinations were performed in triplicate in at least two experiments. Results were analyzed with FloJo version 6.0 (Tree Star).

All data are represented as average ± SE of the mean. Data were analyzed by a two-tailed nonpaired *t* test.

RESULTS

BLOC-1 Is Present in AP-3–derived Vesicles

BLOC-1 and AP-3 complexes are involved in the biogenesis of lysosomes and lysosome-related organelles (Li *et al.*, 2004; Di Pietro and Dell'Angelica, 2005), yet the mechanisms by which these complexes participate in organelle biogenesis remain unexplored. To understand functional relationships between AP-3 and BLOC-1 complexes, we analyzed whether similar stages or molecules involved in AP-3–dependent vesicle transport were similarly affected by BLOC-1 and AP-3 deficiencies.

We first determined whether BLOC-1 and AP-3 complexes were found on the same vesicle population. Mass spectrometry analysis of AP-3–containing microvesicles suggested the presence of the BLOC-1 complex subunits, dysbindin, snapin, pallidin, and muted. These BLOC-1 subunit polypeptides were represented by a cumulative count of 17 peptides (Figure 1A). Much like the AP-3 complex (Salazar *et al.*, 2005b), BLOC-1 complex subunit peptides were independently identified in different vesicle preparations/mass spectrometry rounds (Figure 1A). To confirm the presence of BLOC-1 complex subunits in AP-3–containing

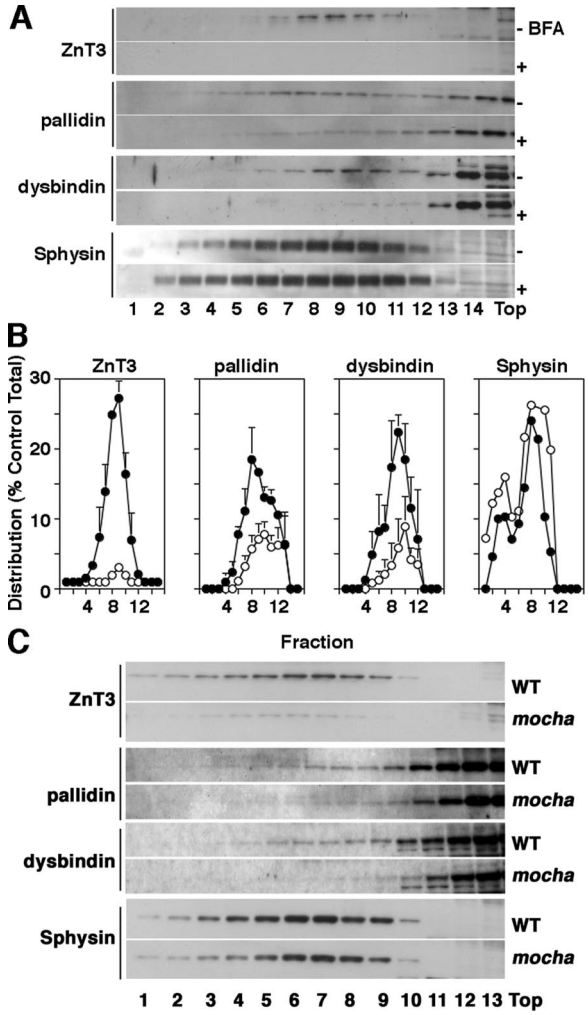

Figure 2. BLOC-1 subunits are present in AP-3–derived vesicles. (A) PC12 cells were treated in either the absence or presence of brefeldin A (BFA) to deplete AP-3–generated vesicles. Microvesicles were obtained by sedimentation in glycerol velocity gradients. Synaptophysin levels were not affected by brefeldin A. In contrast, the levels of ZnT3 and the BLOC-1 subunits dysbindin and pallidin were reduced (n = 3). (B) Normalized content distribution of the antigens presented in A (n = 3). (●), vesicles isolated from untreated PC12 cells; (○), vesicles isolated from brefeldin A–treated cells. (C) High-speed supernatants (S2) from wild-type (WT) and *mocha* brain homogenates were fractionated in glycerol gradients to resolve synaptic vesicle–containing fractions. Synaptic vesicle antigen levels across gradients were determined by immunoblot using antibodies against: ZnT3, pallidin, dysbindin, and synaptophysin (Sphysin). BLOC-1 subunits and ZnT3 antigen content in membranes were specifically altered in *mocha* brain vesicles.

microvesicles, we performed immunomagnetic isolation of glycerol gradient–purified PC12 microvesicles, a membrane fraction enriched in AP-3–containing microvesicles (Salazar *et al.*, 2005b). Beads coated with either human specific LAMP1, AP-1 γ-subunit, or AP-2 α-subunit antibodies were used as negative controls. Membrane binding was negligible to control beads as determined with antibodies against the integral membrane protein ZnT3, an AP-3–interacting cargo (Figure 1B, compare lanes 1–3 and 4; Salazar *et al.*, 2004b). In contrast, ZnT3-containing microvesicles were enriched by beads decorated with AP-3 delta antibodies. ZnT3 microvesicles isolated with AP-3 delta antibodies contained

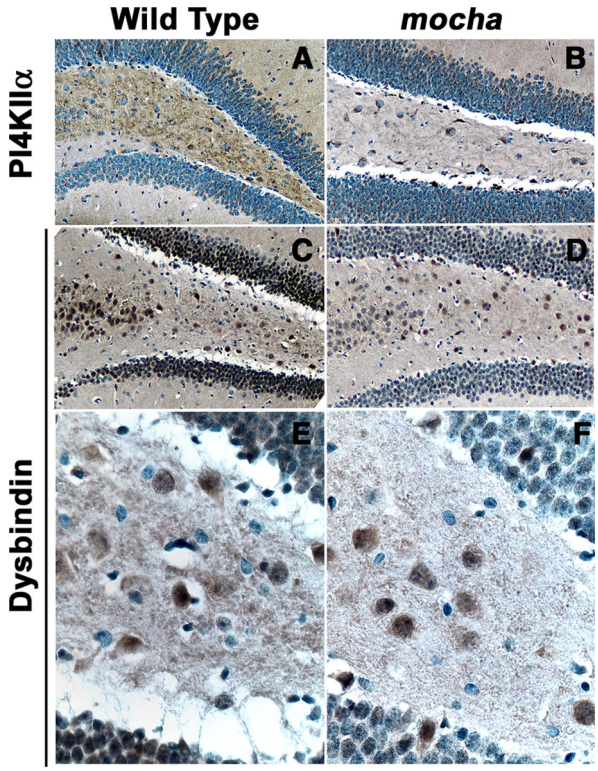

Figure 3. Dysbindin content decreases in *mocha* hippocampal mossy fiber nerve terminals. Wild-type (A, C, and E) and *mocha* (B, D, and F) hippocampal brains sections were stained with antibodies against phosphatidylinositol-4-kinase type II alpha (PI4KIIα, A and B) and dysbindin (C–F). Immunocomplexes were detected with the ABC peroxidase reagent and DAB deposition. (A–D) Representative images of the dentate gyrus and hilus at low (A–D, 20×) and high magnification (E and F, 63×; n = 2).

β3-adaptin as well as dysbindin and pallidin, thus indicating that these organelles possessed AP-3 and BLOC-1, respectively.

To further explore the presence of BLOC-1 subunits in AP-3–derived microvesicles, we used pharmacological and genetic tools that abrogate AP-3 microvesicle formation. PC12 cell microvesicles are generated from both endosomes and the plasma membrane by AP-3– and AP-2–dependent mechanisms, respectively (Shi *et al.*, 1998; Blagoveshchenskaya *et al.*, 1999; Hannah *et al.*, 1999; Salazar *et al.*, 2004b, 2005b). Importantly, the AP-3 pathway is sensitive to brefeldin A (Shi *et al.*, 1998; Blagoveshchenskaya *et al.*, 1999; Salazar *et al.*, 2004b, 2005b), and it can be assessed by analyzing ZnT3 (Salazar *et al.*, 2004b, 2005b). In contrast, the plasma membrane route is insensitive to brefeldin A, and it can be monitored via the synaptic vesicle protein synaptophysin (Thiele *et al.*, 2000; Salazar *et al.*, 2004b, 2005b). We hypothesized that if BLOC-1 subunits are contained in AP-3 microvesicles, the presence of BLOC-1 subunits in PC12 microvesicles should be sensitive to brefeldin A. To test this hypothesis, PC12 cells were treated in the absence or presence of brefeldin A and microvesicles were isolated by differential and glycerol gradient velocity sedimentation (Figure 2, A and B). Gradient fractions were analyzed for the presence of ZnT3, BLOC-1 subunits, and synaptophysin. AP-3 microvesicles (Figure 2, A–C) peak in the middle of glycerol gradients, whereas soluble cytosolic proteins remain at the top gradient fractions. As previously described by us, brefeldin A substantially decreased ZnT3 content in PC12 microvesicle-containing fractions (Figure 2, A and B) while sparing vesicles enriched in synaptophysin (Sphysin, Figure 2, A and B). Moreover and much like ZnT3, the targeting of BLOC-1 subunits pallidin and dysbindin to microvesicles was sensitive to brefeldin A, thus suggesting that BLOC-1 complex subunits are present on AP-3–derived

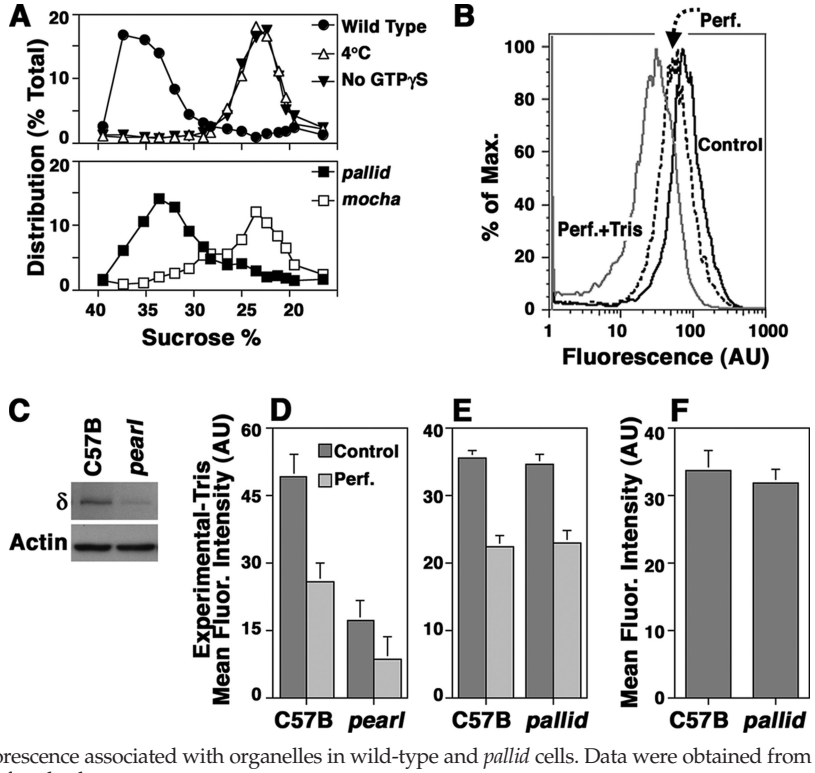

Figure 4. BLOC-1 deficiency does not affect AP-3 binding to membranes. (A) PC12 VAMP2-N49A microvesicles were incubated with wild-type cytosol either in the absence (▼) or presence of 20 μM GTPγS (●; Faundez *et al.*, 1998). Cytosol- and GTPγS-treated vesicles increased their sedimentation to 34% sucrose. Membrane density shift was abrogated in reactions performed with wild-type cytosol and GTPγS maintained at 4°C (Δ) or in reactions performed at 37°C in the presence of GTPγS but instead in the presence of cytosol isolated from AP-3–deficient *mocha* brains (□). Cytosol from BLOC-1–deficient *pallid* brain was indistinguishable from wild type (■; n = 2). (B) PC12 cell were treated in intracellular buffer either in the absence (control) or presence of saponin (Perf., perforated) to release cytosolic proteins. Membrane bound adaptors were stripped by further treating perforated cells with Tris, 0.5 M (Perf.+Tris). Cells were fixed and stained with antibodies against the delta subunit of AP-3. Fluorescence intensity was determined by flow cytometry. (C) Immunoblot analysis of the AP-3 levels in wild-type (C57B) and *pearl* cells. (D) Flow cytometry analysis of the AP-3 levels present in control nonperforated cells and saponin-perforated wild-type and *pearl* cells. (E) Flow cytometry analysis of the AP-3 levels in control nonperforated cells and saponin-perforated wild-type and *pallid* cells. Experiments depicted in D and E were performed in triplicate in three independent experiments using three cell isolates of each genotype. Specific cell fluorescence was obtained after subtracting the fluorescence present in Tris-treated cells. (F) Metamorph determination of the AP-3 delta immunofluorescence associated with organelles in wild-type and *pallid* cells. Data were obtained from 38 wild-type and 37 *pallid* cells using three cell isolates of each phenotype.

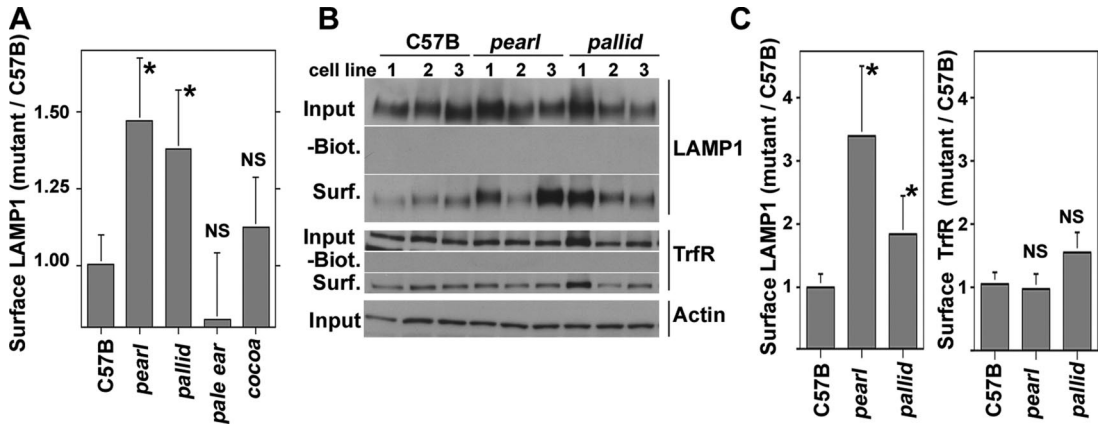

Figure 5. Surface levels of LAMP1 are altered in AP-3– and BLOC-1–deficient fibroblasts. (A) Fixed cells were stained for LAMP1 in absence of detergent to assess surface staining. Mean fluorescence intensity was analyzed by flow cytometry, and staining was normalized by subtracting the mean fluorescence values of stainings lacking primary antibodies. Results are expressed as the ratio of the mean fluorescence intensity obtained from mutant and wild-type fibroblasts (C57B). All determinations were performed in triplicate assays, in two independent experiments using three cell isolates of each genotype. (B) Fibroblasts were surface biotinylated, lysed, and biotinylated proteins isolated with streptavidin beads. Precipitated proteins or 5% of input were blotted for either LAMP1, the transferrin Receptor (TrfR), or actin as a loading control. (C) Depicts the quantification of LAMP1 and transferrin receptor surface levels presented in B. All experiments were performed in duplicate, in two independent experiments using three distinct cell isolates per each genotype. Asterisks indicate average ± SEM. NS, nonsignificant differences.

microvesicles and/or that the BLOC-1 complex is recruited to membranes by an ARF-dependent mechanism. To discern between these possibilities, we analyzed the content of BLOC-1 subunits pallidin and dysbindin in microvesicles isolated from wild-type and AP-3–deficient *mocha* brains, the latter lacking ZnT3-microvesicles (Figure 2C). Similar to the behavior observed in brefeldin A–treated PC12 cells, AP-3-null brain microvesicle fractions possessed reduced levels of ZnT3, pallidin, and dysbindin; yet, their synaptophysin content remained mostly unaffected (Figure 2C). We confirmed the *mocha* brain subcellular fractionation results by analyzing the distribution of BLOC-1 in brain tissue sections (Figure 3). A hallmark of proteins targeted to brain AP-3 microvesicles is that their content is reduced in dentate gyrus mossy fibers in AP-3–deficient *mocha* nerve terminals (Salazar *et al.*, 2004a, 2005b). This AP-3 null histological phenotype correlates with the mistargeting of these proteins to brain vesicles (Salazar *et al.*, 2004a, 2005b). To assess the distribution of BLOC-1 complex in hippocampus, we stained mouse brain sections from control and AP-3–deficient *mocha* mouse brains with antibodies against dysbindin (Figure 3, C–F) and phosphatidylinositol-4-kinase type II alpha (Figure 3, A and B), a kinase whose levels are reduced in *mocha* mossy fiber nerve terminals and synaptic vesicle fractions. Antigen–antibody complexes were revealed using a peroxidase-based detection system that generates a dark brown precipitate. Dysbindin staining was prominent in the dentate gyrus of the hippocampus both in cell bodies and nerve terminals, following a pattern and distribution similar to the dysbindin staining already reported in human hippocampus (Figure 3, C and E; Talbot *et al.*, 2004). Importantly, the mossy fiber nerve terminal dysbindin immunoreactivity was reduced in AP-3–deficient dentate gyrus (Figure 3, D and F). This dysbindin behavior in mossy fiber nerve terminals is similar to phosphatidylinositol-4-kinase type II alpha, an AP-3 cargo molecule (compare Figure 3, A and B; Salazar *et al.*, 2005b). Collectively; mass-spectrometry, biochemical, pharmacological, genetic, and histological approaches support the hypothesis that the BLOC-1 complex subunits coexist in vesicles either generated by or containing the adaptor complex AP-3.

BLOC-1 Deficiency Does Not Affect AP-3 Binding to Membranes

The presence of BLOC-1 complexes in vesicles containing AP-3, the similar phenotypes observed in mice deficient in either AP-3 or BLOC-1 subunits (Li *et al.*, 2004; Di Pietro and Dell'Angelica, 2005), and the genetic interaction of AP-3 and BLOC-1 complexes (Gautam *et al.*, 2006) suggests a role of BLOC-1 complexes in either regulating AP-3 recruitment to membranes and/or the sorting of AP-3 cargoes. We first tested whether AP-3 recruitment to membranes was affected in the absence of BLOC-1 complexes using a cell-free assay (Figure 4A; Faundez *et al.*, 1998). These studies were complemented by the analysis of the steady-state levels of membrane-bound AP-3 in whole cells (Figure 4, B–F).

Isolated PC12 cell microvesicles can be coated in a cell-free system by a mechanism that selectively depends on AP-3 and ARF-GTP (Faundez *et al.*, 1998). No other coats are recruited to these microvesicles (Faundez *et al.*, 1998). Furthermore, this coating mechanism is saturable (Faundez *et al.*, 1998) and purified AP-3 and ARF1-GTP are sufficient to induce microvesicle coating of the same magnitude as with brain cytosol (unpublished results). Vesicle coating by AP-3 is manifested as a change in vesicle density (Faundez *et al.*, 1998; Blumstein *et al.*, 2001). Glycerol-isolated PC12 cell microvesicles were incubated with wild-type cytosol either in the absence (▼) or presence of GTPγS (●) to induce coat recruitment (Figure 4A). Cytosol and GTPγS-treated vesicles increased their sedimentation from 22 to 34% sucrose, indicating coat recruitment. Membrane density shift was abrogated in reactions performed with wild-type cytosol and GTPγS but maintained at 4°C (Δ) or in reactions performed at 37°C in the presence of GTPγS but instead supplemented with AP-3–deficient *mocha* cytosol (□), demonstrating the dependence of this assay on AP-3 (Faundez *et al.*, 1998; Blumstein *et al.*, 2001). Importantly, microvesicle coating reactions performed in the presence of BLOC-1–deficient

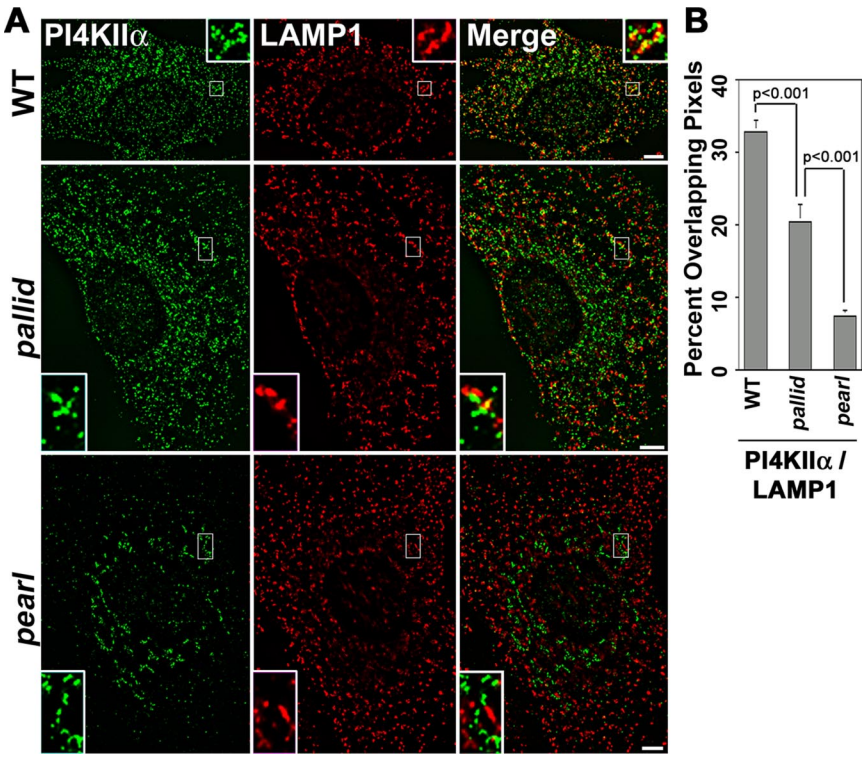

Figure 6. The *pearl* and *pallid* alleles alter phosphatidylinositol-4-kinase type II alpha subcellular distribution. (A) Wild-type, AP-3–deficient *pearl*, and BLOC-1–deficient *pallid* cells were costained with antibodies against phosphatidylinositol-4-kinase type II alpha (PI4KIIα) and LAMP1. Cells were imaged by wide-field deconvolution microscopy, and the extent of signal overlap between phosphatidylinositol-4-kinase type II alpha and LAMP1 was determined using Metamorph software (B). Data were obtained from 11 wild-type cells (WT), 12 *pallid* cells, and 5 *pearl* cells. Three independent cell isolates were analyzed per genotype. No significant differences in signal overlap among cell isolates of the same genotype were detected. Insets are threefold magnification of a representative region of the cell (Bar, 5 μm).

pallid cytosol (Figure 4A, ■) were indistinguishable from those generated with wild-type cytosol, suggesting that the BLOC-1 complex is not necessary for ARF-dependent AP-3 recruitment to membranes.

AP-3 binding to organelles could be regulated by BLOC-1 at a later stage after vesicle scission, like, for example, during vesicle uncoating by modifying the amount of AP-3 bound to membranes. We studied this possibility by analyzing the steady-state organelle-bound AP-3 content using AP-3 delta cell staining and fluorescence intensity determination by flow cytometry (Figure 4, B–E). Staining was performed in whole cells to assess total adaptor levels, in cells perforated in intracellular buffer (perf.) to remove nonmembrane associated cytosolic AP-3, and in cells perforated in the presence of 0.5 M Tris, pH 8 (perf.+Tris), a condition that removes membrane-bound adaptors (Figure 4B; Chang *et al.*, 1993). Cell perforation in intracellular buffer decreased fluorescence intensity to ~50% of the total AP-3 content, yet perforation in the presence of Tris decreased fluorescence intensity threefold (Figure 4B). The mean fluorescence intensity of Tris-treated perforated cells was identical whether wild-type or AP-3–deficient *pearl* cells were analyzed, therefore, indicating that fluorescence remaining after Tris treatment corresponded to a background signal (unpublished data). We further validated the flow cytometry assay by testing whether it could detect differences in AP-3 levels between wild-type and AP-3–deficient *pearl* cells (Figure 4, C and D). The *pearl* mutation is a hypomorphic allele of the *Ap3b1* locus and low AP-3 levels remains in these cells (Figure 4C; Yang *et al.*, 2000; Peden *et al.*, 2002). This small AP-3 pool was detected in *pearl* cells, a result consistent with our blot determination and previous findings (Figure 4D; Yang *et al.*, 2000; Peden *et al.*, 2002). These results demonstrate that AP-3 flow cytometry distinguishes between membrane-associated and cytosolic AP-3 pools in a genotype-sensitive manner. The effects of the *pallid* mutation on AP-3 pools were explored by flow cytometry (Figure 4E). Neither the total AP-3 levels nor the membrane bound pools were affected by the lack of functional BLOC-1 complexes, arguing against a necessary role of BLOC-1 in regulating the steady-state levels of AP-3 on membranes. Because small differences could be obscured by background nonmembrane bound pools of AP-3 in perforated cells, we analyzed the AP-3 fluorescence intensity associated with organelles in intact cells by confocal microscopy and Metamorph quantification of total cell fluorescence (Figure 4F). Similar to the flow cytometry results, we did not detect differences between wild-type and BLOC-1–deficient *pallid* cells, arguing that the steady state levels of membrane-bound AP-3 are not affected in *pallid* cells. Thus, a diverse set of cell-free and whole cell approaches indicate that AP-3 recruitment and membrane-bound steady state levels of AP-3 are unaffected by the absence of BLOC-1 complexes.

AP-3 and BLOC-1 Regulate the Targeting of AP-3 Cargo Proteins

The presence of AP-3 and BLOC-1 subunits on the same organelle suggests that BLOC-1 complexes could regulate the targeting of AP-3 cargoes at a step downstream of AP-3 recruitment. We examined whether known sorting phenotypes observed in AP-3–null cells could be recapitulated either completely or partially in BLOC-1–deficient cells. We focused on two well-documented AP-3 cargo membrane proteins, LAMP1 and phosphatidylinositol-4-kinase type II alpha, whose distribution is altered in AP-3-null cells (Bonifacino and Traub, 2003; Salazar *et al.*, 2005b). LAMP1 and phosphatidylinositol-4-kinase type II alpha phenotypes were explored in three independent cell isolates of immortalized skin fibroblasts obtained from either AP-3– (*pearl*) or BLOC-1–deficient (*pallid*) mice. An identical number of C57B (wild type), BLOC-2– (*cocoa*), and BLOC-3–deficient (*pale ear*) mouse fibroblast isolates were used as controls.

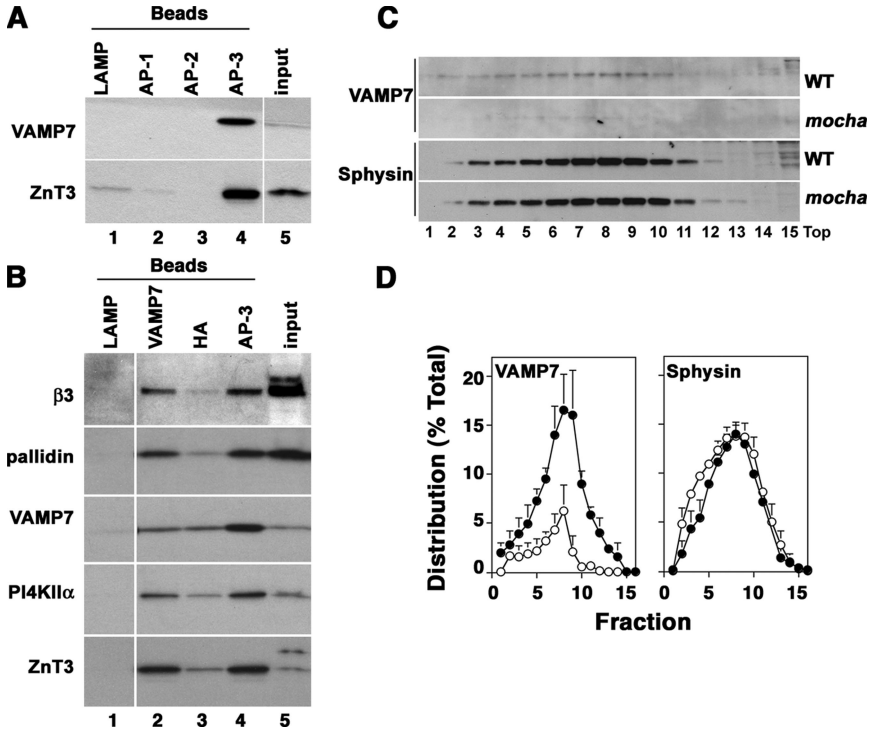

Figure 7. VAMP7-TI is present in AP-3 microvesicles. (A) Glycerol gradient-purified PC12 microvesicles were bound to magnetic beads coated with either human-specific LAMP1 (lane 1), AP-1 γ-subunit (lane 2), AP-2 α-subunit antibodies (lane 3), or AP-3 delta adaptin monoclonal antibodies (lane 4). Bead bound vesicles were resolved by SDS-PAGE and analyzed by immunoblot with antibodies against ZnT3 and VAMP7-TI (VAMP7). (B) Purified PC12 microvesicles were bound to magnetic beads coated with either human-specific LAMP1 (lane 1), VAMP7-TI (lane 2), HA tag to recognize the HA epitope engineered in ZnT3 (lane 3), or AP-3 delta adaptin monoclonal antibodies (lane 4). Complexes were analyzed by immunoblot as in A with antibodies against β3B adaptin (β3), pallidin, VAMP7-TI (VAMP7), phosphatidylinositol-4-kinase type II alpha (PI4KIIα), and ZnT3. (A and B) Input represents 10% of the vesicles used per assay. (C) High-speed supernatants (S2) from wild-type and *mocha* brain homogenates were fractionated in glycerol gradients to resolve synaptic vesicles and AP-3 vesicles. Antigen levels across gradients were determined by immunoblot using antibodies against VAMP7-TI (VAMP7) and synaptophysin (Sphysin). (D) Depicts the normalized content distribution of the antigens presented in B (n = 3).

We first analyzed targeting of LAMP1, an AP-3–interacting membrane protein (Figure 5; Bonifacino and Traub, 2003). Increased LAMP1 surface expression is a well-documented phenotype of AP-3 deficiencies either affecting the β3 (*pearl*; Dell'Angelica *et al.*, 1999; Peden *et al.*, 2002), δ (*mocha*; Peden *et al.*, 2004; Styers *et al.*, 2004), or μ3 subunits of AP-3 (Le Borgne *et al.*, 1998; Janvier and Bonifacino, 2005). Cell surface LAMP1 was measured by flow cytometry using luminal antibodies against the mouse antigen (Figure 5A). AP-3–deficient *pearl* cells increased their surface LAMP1 content when compared with wild-type cells (1.47 ± 0.2-fold increase, $p < 0.013$, n = 6 per cell isolate). The magnitude of this increase in plasma membrane levels is similar to previously reported findings (Dell'Angelica *et al.*, 1999; Peden *et al.*, 2002). Furthermore and consistent with our hypothesis, the LAMP1 surface content was significantly increased in BLOC-1–deficient *pallid* cells over wild-type cells (Figure 5A, 1.37 ± 0.18-fold increase, $p < 0.022$, n = 6 per cell isolate). Importantly, LAMP1 surface levels in BLOC-2– (*cocoa*, 1.12 ± 0.16, $p = 0.222$, n = 6 per cell isolate) and BLOC-3–deficient (*pale ear*, 0.82 ± 0.21, $p = 0.189$, n = 6 per cell isolate) fibroblasts were not significantly different from those found in wild-type cells (Figure 5A). These results are consistent with a selective targeting phenotype restricted to AP-3 and BLOC-1 deficiencies.

Cell surface–selective biotinylation of LAMP1 followed by immunoblot analysis was used as a second way to examine how AP-3 and BLOC-1 deficiencies affect the traffic of this lysosomal protein. Transferrin receptor was used as a control because its sorting and cell surface levels remain unaltered in AP-3 deficiencies (Dell'Angelica *et al.*, 1999; Peden *et al.*, 2004; Styers *et al.*, 2004; Janvier and Bonifacino, 2005). Consistent with the flow cytometry results, the surface content of LAMP1 was increased in AP-3–deficient *pearl* and BLOC-1–deficient *pallid* cells (Figure 5, B and C, *pearl*, 3.4 ± 1.1-fold increase, $p < 0.0035$, n = 4 per cell isolate; *pallid*, 1.85 ± 0.5-fold increase, $p < 0.0035$, n = 4 per cell isolate). The *pallid* LAMP1 surface phenotype determined by surface biotinylation was intermediate to the one seen in AP-3 mutant cells. The effects of the *pearl* and *pallid* alleles on LAMP1 were selective for AP-3–targeted proteins because transferrin receptor surface levels were not significantly different from those observed in wild-type cells (Figure 5, B and C).

We further explored membrane protein sorting in AP-3 and BLOC-1 deficiencies by analyzing the subcellular distribution of another AP-3 cargo protein, phosphatidylinositol-4-kinase type II alpha. Subcellular localization of the kinase is perturbed in brain and primary cultures from the AP-3–null *mocha* mouse (Salazar *et al.*, 2005b). In fibroblasts, the defect is characterized by a lack of targeting of phosphatidylinositol-4-kinase type II alpha to LAMP1–positive organelles (Salazar *et al.*, 2005b). This phenotype is due to a relocalization of the kinase away from LAMP1-positive organelles whose intracellular distribution remains unaltered in AP-3–deficient cells (Dell'Angelica *et al.*, 1999; Yang *et al.*,

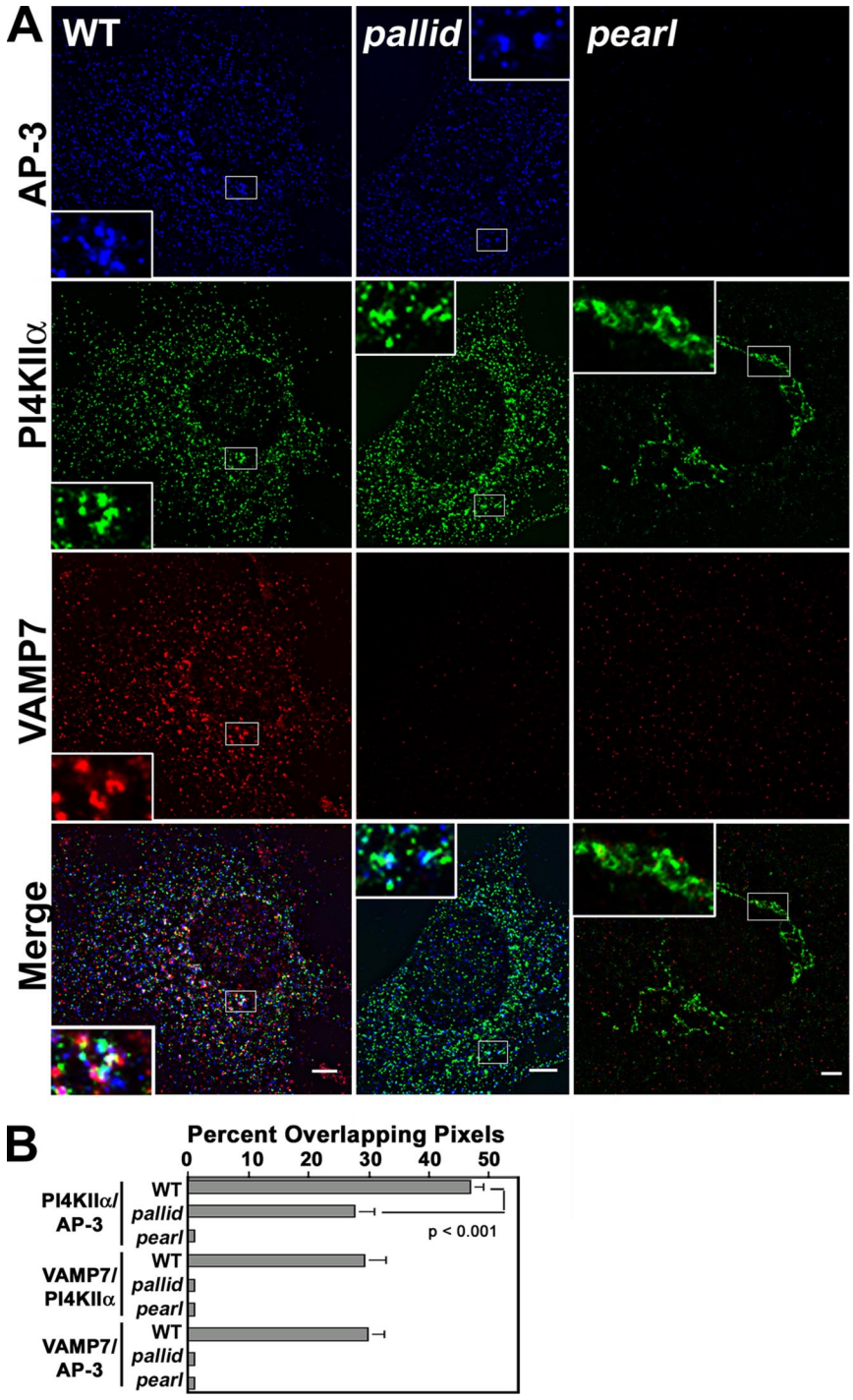

Figure 8. Subcellular localization of AP-3 and AP-3 cargoes in BLOC-1 and AP-3 mutant cells. (A) Wild-type, AP-3–deficient *pearl*, and BLOC-1–deficient *pallid* cells were costained with antibodies against AP-3 delta adaptin and the AP-3 cargoes phosphatidylinositol-4-kinase type II alpha (PI4KIIα) and VAMP7-TI (VAMP7). Cells were imaged by wide-field deconvolution microscopy and the extent of signal overlap between phosphatidylinositol-4-kinase and AP-3, VAMP7-TI and the kinase, and VAMP7-TI and AP-3 were determined using Metamorph software (B). Data were obtained from 9 wild-type cells (WT), 18 *pallid* cells, and 9 *pearl* cells. Three independent cell isolates were analyzed per genotype. No significant differences in overlap among cell isolates of the same genotype were detected. Insets are threefold magnification of a representative region of the cell. Bar, 5 μm.

2000). High-resolution deconvolution immunomicroscopy revealed a similar phenotype in cells carrying another AP-3 mutant allele, *pearl*. *pearl* fibroblasts displayed minimal overlap between phosphatidylinositol-4-kinase type II alpha and LAMP1 (Figure 6, A and B, 7.3 ± 0.85%, 3 cell isolates, n = 5). In contrast, one third of all the kinase-positive puncta overlapped with LAMP1 in wild-type cells (Figure 6, A and B, 32.8 ± 1.6%, 3 cell isolates, n = 11). BLOC-1–deficient cells (*pallid*) presented a phenotype intermediate to the one observed in AP-3–deficient cells, where only one fifth of kinase positive puncta were also immunoreactive for LAMP1 (Figure 6, A and B, 20.4 ± 2.2%, 3 cell isolates, n = 12). Similar results were obtained when the distribution of phosphatidylinositol-4-kinase type II alpha was assessed in the context of AP-3–positive structures (see Figure 8, A and B). Kinase and AP-3 immunoreactivity co-occurred in the same puncta in almost half of the cases (46.9 ± 2.2%, 3 cell isolates, n = 9), yet in *pallid* cells less than one third of the kinase-positive structures were also positive for AP-3 (27.5 ± 3.4%, 3 cell isolates, n = 18, $p < 0.001$). These results support the notion that in the absence of BLOC-1 the kinase is missorted away from LAMP1- and AP-3–positive structures. These results indicate that AP-3 and BLOC-1 genetic deficiencies selectively affect the sorting

of the AP-3 cargo molecules, LAMP1 and phosphatidylinositol-4-kinase type II alpha.

AP-3 and BLOC-1 Deficiencies Selectively Affect the Targeting of VAMP7-TI

The R-(v)-SNARE VAMP7-TI interacts with AP-3 (Martinez-Arca *et al.*, 2003), and it was identified in the AP-3 vesicle proteome together with the BLOC-1 complex subunits and phosphatidylinositol-4-kinase type II alpha (Salazar *et al.*, 2005b), thus suggesting that VAMP7-TI targeting could also be affected by AP-3 and BLOC-1 deficiencies. As a first step, we confirmed whether VAMP7-TI was present in AP-3–positive organelles using biochemical (Figure 7) and immunomicroscopy approaches (Figure 8). Immunomagnetic isolation of AP-3–coated vesicles was performed with beads decorated with antibodies directed against human LAMP1, AP-1 gamma, or AP-2 alpha adaptin as controls (Figure 7A, lanes 1–3). Membrane binding to these beads was negligible as determined by the absence of ZnT3 and VAMP7-TI (Figure 7A, compare lanes 1–3 and 4). However, both of these proteins were present in microvesicles isolated with beads coated with AP-3 delta-adaptin antibodies (Figure 7A, lane 4). Moreover, microvesicles isolated with magnetic beads coated with antibodies against either VAMP7-TI, the HA tag present in ZnT3, or delta adaptin (Figure 7B, lanes 2, 3, and 4, respectively) contained phosphatidylinositol-4-kinase type II alpha and the BLOC-1 subunit pallidin.

We further confirmed the presence of VAMP7-TI on AP-3–generated vesicles from brain. Glycerol gradient–isolated vesicles from wild-type and AP-3–deficient *mocha* brain were analyzed by immunoblot with antibodies against VAMP7-TI and synaptophysin as a control (Figure 7, C and D). Consistent with the presence of VAMP7-TI in AP-3–coated microvesicles, VAMP7-TI content was decreased in microvesicles isolated from AP-3–deficient brain. This effect was selective because synaptophysin content in glycerol gradient–isolated vesicles remained unaffected in the absence of AP-3 (Figure 7, C and D). Because VAMP7-TI and phosphatidylinositol-4-kinase type II alpha reside in microvesicles containing AP-3 and BLOC-1 complexes (see Figure 7, A and B), we determined whether these antigens were present in similar structures in mouse skin fibroblasts. Immunostaining with BLOC-1 subunit antibodies could not be performed because of lack of antibodies appropriate for immunofluorescence (unpublished results). We confirmed the presence of VAMP7-TI in puncta also positive for phosphatidylinositol-4-kinase type II alpha and AP-3 in mouse fibroblast derived from wild-type C57B mice, which was similar to that in AP-3 microvesicles isolated from PC12 cells (Figure 8). Fibroblasts were triple-labeled with antibodies against AP-3 delta, phosphatidylinositol-4-kinase type II alpha, and VAMP7-TI. The degree of overlap between different antibody signals was examined by deconvolution microscopy, and the percent of overlapping pixels per cell was determined by Metamorph analysis. A substantial pool of the AP-3–containing organelles also contained VAMP7-TI and the AP-3 cargo/regulator phosphatidylinositol-4-kinase type II alpha (seen as white structures in Figure 8A). Indeed, one third of all VAMP7-TI–positive puncta contained AP-3 (Figure 8B, 29.7 ± 2.8%, 3 cell isolates, n = 9) and phosphatidylinositol-4-kinase type II alpha (Figure 8B, 29.4 ± 3.3%, 3 cell isolates, n = 9). The extent of overlap between VAMP7-TI and the kinase is similar to that found between the AP-3 cargo proteins LAMP1 and phosphatidylinositol-4-kinase type II alpha (see Figure 6B). Surprisingly, VAMP7-TI staining was below the microscopy detection level in AP-3–deficient *pearl* cells and BLOC-1–deficient *pallid* cells. We confirmed these results by immunoblot analysis of wild-type, *pearl*, and *pallid* cell extracts (Figure 9A). VAMP7-TI total cellular levels were reduced to 42.9 ± 2.8% (n = 6, three cell isolates, $p < 0.0001$) and 59.7 ± 1.3% (n =

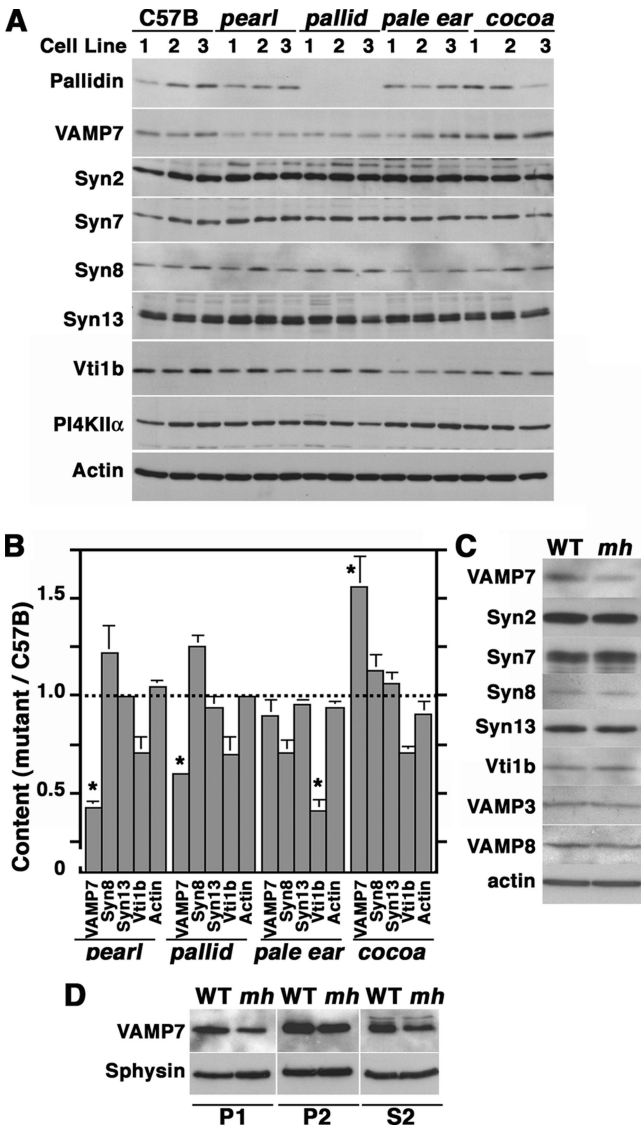

Figure 9. Characterization of the SNARE cellular content in BLOC-1 and AP-3 mutant cells. (A) Equal amounts of wild-type (C57B), AP-3–deficient *pearl*, BLOC-1–deficient *pallid*, BLOC-2–deficient *cocoa*, and BLOC-3–deficient *pale ear* cell extracts were resolved by SDS-PAGE and analyzed by immunoblot with antibodies against pallidin, VAMP7-TI (VAMP7), several syntaxin isoforms (syn2, 7, 8, and 13), Vti1b, phosphatidylinositol-4-kinase type II alpha (PI4KIIα), and β-actin as a loading control. All determinations were performed in triplicate in two independent experiments. (B) Depicts quantification of representative results presented in A. (C) Equal amounts of wild-type and AP-3–deficient *mocha* cell extracts were resolved by SDS-PAGE and analyzed by immunoblot with antibodies against VAMP7-TI (VAMP7), several syntaxin isoforms (syn2, 7, 8, and 13), VAMP3, VAMP8, Vti1b, and β-actin as a loading control (n = 2). (D) Immunoblot analysis of primary brain subfractions P1, P2, and S2 derived from wild-type (WT) and mocha (mh) brains (see *Material and Methods*) using antibodies against VAMP7-TI and synaptophysin (Sphysin) as control. In all AP-3– and BLOC-1–deficient cells or tissues, VAMP7-TI levels are selectively reduced.

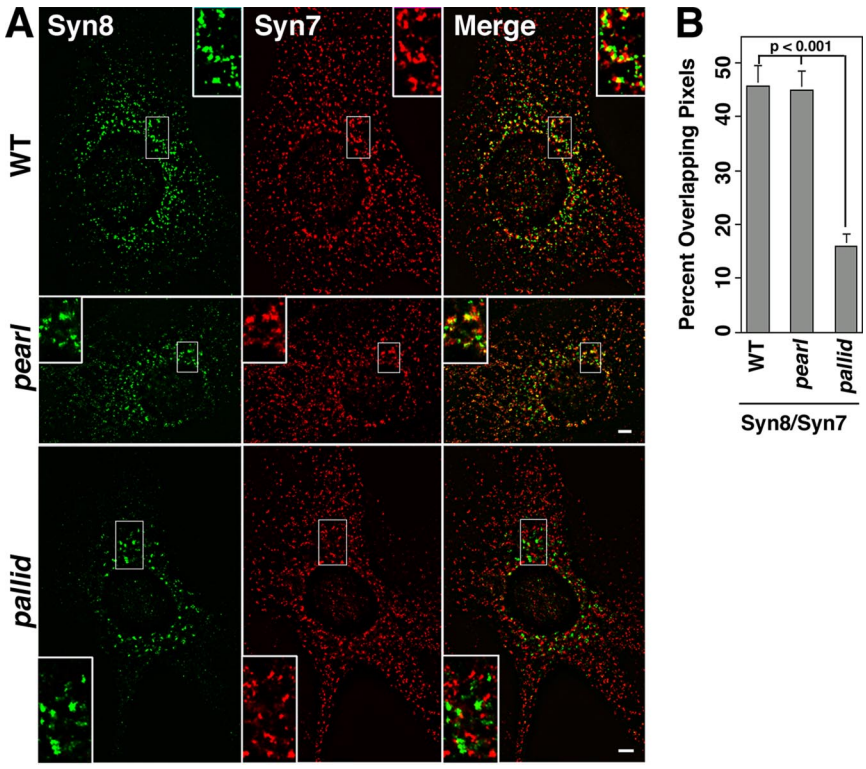

Figure 10. The BLOC-1–deficient *pallid* allele affects the subcellular distribution of syntaxin 8 and 7. (A) Wild-type, AP-3–deficient *pearl*, and BLOC-1–deficient *pallid* cells were costained with antibodies against syntaxin 8 and 7. Cells were imaged by wide-field deconvolution microscopy, and the extent of signal overlap between syntaxin 8 and 7 was determined using Metamorph software (B). Data were obtained from 9 wild-type cells (WT), 8 *pallid* cells, and 8 *pearl* cells. Three independent cell isolates of wild-type and *pearl* cells were analyzed per genotype except for *pallid*, where two cell isolates were analyzed. No significant differences in signal overlap among cell isolates of the same genotype were detected. Insets are threefold magnification of a representative region of the cell. Bar, 5 μm.

9, three cell isolates, $p < 0.0001$) of the controls values in *pearl* and *pallid* cells, respectively (Figure 9B). VAMP7-TI content was not significantly different from wild-type in BLOC-3–deficient cells (*pale ear*, 89.4 ± 8.7%, three cell isolates, $n = 9$, $p = 0.241$), whereas in BLOC-2–deficient cells VAMP7-TI levels were increased when compared with control cells (*cocoa*, 156 ± 15.7%, three cell isolates, $n = 9$, $p < 0.0026$). These results provide evidence that the reduction in VAMP7-TI levels is restricted to AP-3 and BLOC-1 complex deficiencies.

To further explore whether these effects were selective for VAMP7-TI, we determined whether AP-3 and BLOC-1 deficiencies could affect the content of other SNARE complexes (Figure 9, A and B). We focused on cognate pairs of VAMP7-TI (syntaxin 7, 8, and Vti1b; Ward *et al.*, 2000; Bogdanovic *et al.*, 2002; Pryor *et al.*, 2004) and SNAREs reported to interact with pallidin (syntaxin 13; Huang *et al.*, 1999; Moriyama and Bonifacino, 2002), as well as SNAREs unrelated to VAMP7-TI or the endo-lysosomal pathway (syntaxin 2; Hong, 2005). The cellular levels of all these SNARES were not significantly affected in either AP-3– or BLOC-1–deficient cells. Interestingly the levels of Vti1b were significantly reduced only in BLOC-3–deficient cells (*pale ear*, 41.2 ± 5.9%, three cell isolates, $n = 6$, $p < 0.008$) further supporting the observation that effects of AP-3 and BLOC deficiencies on SNAREs were selective. We also analyzed the VAMP7-TI content in AP-3–deficient *mocha* mouse fibroblasts and brain subfractions (Figure 9, C and D). Much like *pearl* and *pallid* cells, *mocha* fibroblasts and brain also possessed selectively reduced VAMP7-TI levels. These results indicate that the AP-3 and BLOC-1 complexes affect the targeting and fate of VAMP7-TI.

The common reduction in the levels of VAMP7-TI observed in AP-3 and BLOC-1–deficient cells could modify the distribution of VAMP7-TI cognate SNARE pairs, syntaxin 7 and syntaxin 8. To test this hypothesis, cells were double-labeled with antibodies against syntaxin 7 and 8, and SNARE distribution was analyzed by high-resolution deconvolution microscopy (Figure 10). In wild-type cells, syntaxin 8, a late endosome SNARE, was predominantly perinuclear where it extensively overlapped with syntaxin 7–positive puncta. In addition, syntaxin 7 was present throughout the cytoplasm, a pattern in agreement with its reported early and late endocytic distribution (Prekeris *et al.*, 1999; Mullock *et al.*, 2000). Almost half of all the syntaxin 8–positive structures overlapped with syntaxin 7 both in wild-type and AP-3–deficient *pearl* cells. In contrast, the overlap of syntaxin 8 and syntaxin 7 signals was reduced to one sixth of the control values in cells lacking BLOC-1 (*pallid*; 15.8 ± 2.9%, $n = 9$, two cell isolates). These results indicate that although AP-3 and BLOC-1 complexes affect the targeting of VAMP7-TI, they diverge in their effect upon VAMP7-TI's cognate Q-(t)-SNAREs.

DISCUSSION

Mutations in loci encoding BLOC-1 subunits recapitulate in part AP-3–deficient phenotypes, suggesting that BLOC-1 and AP-3 operate on the same transport pathway directed toward lysosomes/lysosome-related organelles (Li *et al.*, 2004; Di Pietro and Dell'Angelica, 2005; Gautam *et al.*, 2006). However, before this study the compartments and mechanisms in which AP-3 and BLOC-1 functions converge remained unknown. In this article, we present evidence that the BLOC-1 and AP-3 adaptor complexes coexist on specialized endosomal microvesicles containing AP-3–interacting membrane proteins. We have tested the functionality of the BLOC-1 and AP-3 co-residence in these organelles by demonstrating that BLOC-1 and AP-3 similarly regulate the sorting of membrane proteins targeted by AP-3: LAMP1, phosphatidylinositol-4-kinase type II alpha, and VAMP7-TI.

We identified membrane protein targeting phenotypes characteristic of AP-3 deficiencies in BLOC-1–deficient cells but neither in BLOC-2 or BLOC-3 loss-of-function mutants. Interestingly, LAMP1 and phosphatidylinositol-4-kinase type II alpha mistargeting phenotypes are less pronounced in BLOC-1–deficient cells when compared with AP-3 deficiencies. Previous reports indicated that LAMP1 surface content is affected in AP-3–deficient cells but not in BLOC-1–deficient cells (Dell'Angelica *et al.,* 2000). However, the divergence between previous studies and our present results likely resides in the sensitivity of flow cytometry and surface biotinylation when compared with microscopic assessment of LAMP1 antibody internalization. In addition, we have used three cell isolates of each genotype obtained from primary culture skin fibroblasts. As noted in our experiments, these primary culture–derived cell isolates differ in the endogenous levels of LAMP1 and transferrin receptor despite being derived from the same tissue and possessing the same genotype.

The defective LAMP1 subcellular localization observed in BLOC-1 deficiency is also seen with another AP-3–targeted protein, phosphatidylinositol-4-kinase type II alpha (Salazar *et al.,* 2005b). In this case, the AP-3–deficient phenotype is characterized by a redistribution of the kinase away from peripheral LAMP1-positive organelles and toward a perinuclear region in AP-3–null *mocha* skin fibroblasts (Salazar *et al.,* 2005b). The alteration in the steady state intracellular distribution of LAMP1 is not detectable by fluorescence microscopy in AP-3 deficiencies (Dell'Angelica *et al.,* 1999; Yang *et al.,* 2000), thus allowing the use of LAMP1 as a reference to assess the redistribution of the kinase. Using this technique, we found that the *mocha* kinase redistribution phenotype (Salazar *et al.,* 2005b) is identical in *pearl*-AP-3–deficient cells. Importantly, the overlap of the kinase in LAMP1- or AP-3–positive structures is significantly decreased in BLOC-1–deficient *pallid* cells, yet to a lesser degree when compared with AP-3–deficient cells. Collectively these results provide evidence that AP-3 and BLOC-1 complexes selectively regulate the targeting of AP-3 cargoes.

What is the mechanism by which AP-3 and BLOC-1 functionally associate to regulate AP-3 cargo targeting? We focused on membrane coat recruitment to generate vesicles from donor organelles. The absence of BLOC-1 does not affect the ARF-GTP–dependent recruitment of AP-3 complexes to membranes or organellar AP-3 steady state distribution. However, these data do not rule out the possibility that BLOC-1 may bind to and regulate the recruitment into nascent vesicles of selected cargoes, like SNAREs, either by bridging AP-3 and this type of membrane proteins (accessory adaptor molecule) or by stabilizing specific AP-3-cargo interactions. Defective sorting of SNAREs in AP-3 or BLOC-1 deficiencies could lead primarily to alterations of vesicle membrane fusion, followed by defective targeting of membrane proteins contained in these vesicles. An attractive membrane protein cargo to be controlled by BLOC-1 is the R-(v)-SNARE VAMP7-TI. Like AP-3 and BLOC-1, VAMP7-TI is involved in transport to late endosome/lysosomes (Advani *et al.,* 1999; Ward *et al.,* 2000; Pryor *et al.,* 2004). In addition, VAMP7-TI directly interacts with AP-3 (Martinez-Arca *et al.,* 2003) and is present in organelles positive for AP-3 and other AP-3 cargoes. Moreover, both BLOC-1 and AP-3 bind endocytic SNAREs (Huang *et al.,* 1999; Ilardi *et al.,* 1999; Moriyama and Bonifacino, 2002; Martinez-Arca *et al.,* 2003; Ruder *et al.,* 2005; Tian *et al.,* 2005). Consistent with our hypothesis, deficiencies in BLOC-1 or AP-3 lead to a selective reduction in the vesicular and total VAMP7-TI levels. Neither other R-(v)- nor other Q-(t)-SNAREs total cellular levels are affected in BLOC-1- and AP-3-null cells. The selectivity of the AP-3 and BLOC-1 effects is further supported by the fact that VAMP7-TI total cellular content are not reduced in BLOC-2– or BLOC-3–deficient cells. On the contrary, BLOC-2 deficiencies increase the levels of VAMP7-TI, thus suggesting that AP-3/BLOC-1 and BLOC2 act at distinct stages of a similar pathway.

The reduced levels of VAMP7-TI led us to explore VAMP7-TI cognate Q-(t)-SNAREs: syntaxin 7, 8, and Vti1b (Ward *et al.,* 2000; Bogdanovic *et al.,* 2002; Pryor *et al.,* 2004). The levels of these Q-(t)-SNAREs are not affected by the decreased VAMP7-TI content observed in AP-3–deficient *pearl* and *mocha* cells. However, the overlap of syntaxin 7 and 8 signals was modified in the absence of BLOC-1 complexes but not in AP-3 deficiencies. This observation indicates that not all cellular phenotypes are shared by BLOC-1 and AP-3 deficiencies. Although our results support the hypothesis that AP-3 and BLOC-1 participate in the sorting of AP-3 cargoes including R-(v)-SNAREs, it is likely that these two complexes may also function in alternative sorting mechanisms independent of each other. This hypothesis could explain the divergent phenotypes observed with syntaxin 7 and 8 overlapping in puncta present in AP-3– and BLOC-1–deficient cells. Although speculative, BLOC-1, in an AP-3–independent mechanism, could regulate sorting into vesicles of a restricted group of cargoes, among them Q-(t)-SNAREs and tissue specific cargoes, bound to late endosome-lysosome compartments. This model is consistent with the observation that mice carrying deficiencies in both AP-3 and BLOC-1 complexes possess phenotypes that are more pronounced than those observed in single complex deficiencies, yet the penetrance of these phenotypes varies among tissues (Gautam *et al.,* 2006).

BLOC-1 complex is present in neuronal microvesicles containing synaptic vesicle markers. An outstanding question is what role BLOC-1 plays in synaptic vesicle mechanisms. There are no reports of neurological phenotypes in the classical pigment dilution mouse mutants whose gene products belong to BLOC-1 (Di Pietro and Dell'Angelica, 2005). However, evidence in humans strongly associates genetic polymorphisms in the genes encoding the BLOC-1 subunits *sandy*/dysbindin (Benson *et al.,* 2004; Owen *et al.,* 2005) and *muted* (Straub *et al.,* 2005) with schizophrenia, a disorder that has been hypothesized to emerge from defective presynaptic mechanisms (Mirnics *et al.,* 2000; Honer and Young, 2004). Several intriguing parallels can be drawn between schizophrenia brain analyses and our studies in neuronal cells. First, schizophrenia brain possesses reduced levels of proteins involved in presynaptic vesicle fusion such as VAMP2 and SNAP-25 (Honer *et al.,* 2002; Mukaetova-Ladinska *et al.,* 2002; Halim *et al.,* 2003; Knable *et al.,* 2004), thus suggesting that defective synaptic vesicle fusion mechanisms could contribute to the pathogenesis of this psychiatric disorder. Importantly, and much like the synaptic phenotypes of AP-3–deficient *mocha* mice, there are no changes in the content of the synaptic vesicle protein synaptophysin in schizophrenia brain (Halim *et al.,* 2003) despite reduction in the content of synaptic vesicle SNAREs. A role of BLOC-1 in targeting and fate of fusion machinery components is supported by our findings concerning the R-(v)-SNARE VAMP7-TI as well as by the phenotype of mice deficient in the BLOC-1 subunit SNAPIN. These mice posses impaired neurotransmitter secretion by mechanisms involving the SNARE SNAP-25 (Tian *et al.,* 2005). Second, brain tissue of schizophrenia patients has reduced levels of dysbindin in mossy fibers (Talbot *et al.,* 2004), a phenotype similar to the one found in *mocha* brain. Finally, in conjunction with the reduced levels of dysbindin,

the presynaptic levels of a synaptic vesicle protein sorted in part by AP-3 (Salazar *et al.*, 2005a), the vesicular glutamate transporter 1 (Vglut1), are increased in hippocampal nerve terminals of schizophrenia patients (Talbot *et al.*, 2004). These correlations suggest the attractive possibility that neuronal vesicle targeting and fusion mechanisms regulated by AP-3 and BLOC-1 could contribute to the pathogenesis of complex neuropsychiatric disorders such as schizophrenia.

Collectively, our results support a model where AP-3 and BLOC-1 complexes can either concertedly participate in the same sorting pathway or function in targeting mechanisms independent of each other. Moreover, our findings raise the question of how these novel trafficking mechanisms contribute to neuronal function in normal and disease states.

ACKNOWLEDGMENTS

We are indebted to the Faundez lab members and Dr. S. L'Hernault for his comments. This work was supported by Grant NS42599 from the National Institutes of Health to V.F. and an AHA Beginning Grant-in-Aid to E.W. M.L.S. is a recipient of a NIAMS Research Training Grant (T32) in Dermatology (2 T32 AR007587).

REFERENCES

Advani, R. J., Yang, B., Prekeris, R., Lee, K. C., Klumperman, J., and Scheller, R. H. (1999). VAMP-7 mediates vesicular transport from endosomes to lysosomes. J. Cell Biol. *146*, 765–776.

Benson, M. A., Sillitoe, R. V., and Blake, D. J. (2004). Schizophrenia genetics: dysbindin under the microscope. Trends Neurosci. *27*, 516–519.

Black, M. W., and Pelham, H. R. (2000). A selective transport route from Golgi to late endosomes that requires the yeast GGA proteins. J. Cell Biol. *151*, 587–600.

Blagoveshchenskaya, A. D., Hewitt, E. W., and Cutler, D. F. (1999). Di-leucine signals mediate targeting of tyrosinase and synaptotagmin to synaptic-like microvesicles within PC12 cells. Mol. Biol. Cell *10*, 3979–3990.

Blumstein, J., Faundez, V., Nakatsu, F., Saito, T., Ohno, H., and Kelly, R. B. (2001). The neuronal form of adaptor protein-3 is required for synaptic vesicle formation from endosomes. J. Neurosci. *21*, 8034–8042.

Bogdanovic, A., Bennett, N., Kieffer, S., Louwagie, M., Morio, T., Garin, J., Satre, M., and Bruckert, F. (2002). Syntaxin 7, syntaxin 8, Vti1 and VAMP7 (vesicle-associated membrane protein 7) form an active SNARE complex for early macropinocytic compartment fusion in *Dictyostelium discoideum*. Biochem. J. *368*, 29–39.

Bonifacino, J. S., and Glick, B. S. (2004). The mechanisms of vesicle budding and fusion. Cell *116*, 153–166.

Bonifacino, J. S., and Traub, L. M. (2003). Signals for sorting of transmembrane proteins to endosomes and lysosomes. Annu. Rev. Biochem. *72*, 395–447.

Chang, M. P., Mallet, W. G., Mostov, K. E., and Brodsky, F. M. (1993). Adaptor self-aggregation, adaptor-receptor recognition and binding of alpha-adaptin subunits to the plasma membrane contribute to recruitment of adaptor (AP2) components of clathrin-coated pits. EMBO J. *12*, 2169–2180.

Clift-O'Grady, L., Desnos, C., Lichtenstein, Y., Faundez, V., Horng, J. T., and Kelly, R. B. (1998). Reconstitution of synaptic vesicle biogenesis from PC12 cell membranes. Methods *16*, 150–159.

Dell'Angelica, E. C., Aguilar, R. C., Wolins, N., Hazelwood, S., Gahl, W. A., and Bonifacino, J. S. (2000). Molecular characterization of the protein encoded by the Hermansky-Pudlak syndrome type 1 gene. J. Biol. Chem. *275*, 1300–1306.

Dell'Angelica, E. C., Shotelersuk, V., Aguilar, R. C., Gahl, W. A., and Bonifacino, J. S. (1999). Altered trafficking of lysosomal proteins in Hermansky-Pudlak syndrome due to mutations in the beta 3A subunit of the AP-3 adaptor. Mol. Cell *3*, 11–21.

Di Pietro, S. M., and Dell'Angelica, E. C. (2005). The cell biology of Hermansky-Pudlak syndrome: recent advances. Traffic *6*, 525–533.

Faundez, V., Horng, J. T., and Kelly, R. B. (1997). ADP ribosylation factor 1 is required for synaptic vesicle budding in PC12 cells. J. Cell Biol. *138*, 505–515.

Faundez, V., Horng, J. T., and Kelly, R. B. (1998). A function for the AP3 coat complex in synaptic vesicle formation from endosomes. Cell *93*, 423–432.

Feng, L., *et al.* (1999). The beta3A subunit gene (Ap3b1) of the AP-3 adaptor complex is altered in the mouse hypopigmentation mutant pearl, a model for Hermansky- Pudlak syndrome and night blindness. Hum. Mol. Genet. *8*, 323–330.

Gautam, R., Novak, E. K., Tan, J., Wakamatsu, K., Itoh, S., and Swank, R. T. (2006). Interaction of Hermansky-Pudlak syndrome genes in the regulation of lysosome-related organelles. Traffic *7*, 779–792.

Guo, J., Wenk, M. R., Pellegrini, L., Onofri, F., Benfenati, F., and De Camilli, P. (2003). Phosphatidylinositol 4-kinase type IIalpha is responsible for the phosphatidylinositol 4-kinase activity associated with synaptic vesicles. Proc. Natl. Acad. Sci. USA *100*, 3995–4000.

Gurkan, C., Lapp, H., Alory, C., Su, A. I., Hogenesch, J. B., and Balch, W. E. (2005). Large-scale profiling of Rab GTPase trafficking networks: the membrome. Mol. Biol. Cell *16*, 3847–3864.

Halim, N. D., Weickert, C. S., McClintock, B. W., Hyde, T. M., Weinberger, D. R., Kleinman, J. E., and Lipska, B. K. (2003). Presynaptic proteins in the prefrontal cortex of patients with schizophrenia and rats with abnormal prefrontal development. Mol. Psychiatr. *8*, 797–810.

Hannah, M. J., Schmidt, A. A., and Huttner, W. B. (1999). Synaptic vesicle biogenesis. Annu. Rev. Cell Dev. Biol. *15*, 733–798.

Hirst, J., Miller, S. E., Taylor, M. J., von Mollard, G. F., and Robinson, M. S. (2004). EpsinR is an adaptor for the SNARE protein Vti1b. Mol. Biol. Cell *15*, 5593–5602.

Honer, W. G., Falkai, P., Bayer, T. A., Xie, J., Hu, L., Li, H. Y., Arango, V., Mann, J. J., Dwork, A. J., and Trimble, W. S. (2002). Abnormalities of SNARE mechanism proteins in anterior frontal cortex in severe mental illness. Cereb. Cortex *12*, 349–356.

Honer, W. G., and Young, C. E. (2004). Presynaptic proteins and schizophrenia. Int. Rev. Neurobiol. *59*, 175–199.

Hong, W. (2005). SNAREs and traffic. Biochim. Biophys. Acta *1744*, 493–517.

Huang, L., Kuo, Y. M., and Gitschier, J. (1999). The pallid gene encodes a novel, syntaxin 13-interacting protein involved in platelet storage pool deficiency. Nat. Genet. *23*, 329–332.

Ilardi, J. M., Mochida, S., and Sheng, Z. H. (1999). Snapin: a SNARE-associated protein implicated in synaptic transmission. Nat. Neurosci. *2*, 119–124.

Janvier, K., and Bonifacino, J. S. (2005). Role of the endocytic machinery in the sorting of lysosome-associated membrane proteins. Mol. Biol. Cell *16*, 4231–4242.

Kantheti, P., Diaz, M. E., Peden, A. E., Seong, E. E., Dolan, D. F., Robinson, M. S., Noebels, J. L., and Burmeister, M. L. (2003). Genetic and phenotypic analysis of the mouse mutant mh(2J), an Ap3d allele caused by IAP element insertion. Mamm. Genome *14*, 157–167.

Kantheti, P., *et al.* (1998). Mutation in AP-3 delta in the mocha mouse links endosomal transport to storage deficiency in platelets, melanosomes, and synaptic vesicles. Neuron *21*, 111–122.

Knable, M. B., Barci, B. M., Webster, M. J., Meador-Woodruff, J., and Torrey, E. F. (2004). Molecular abnormalities of the hippocampus in severe psychiatric illness: postmortem findings from the Stanley Neuropathology Consortium. Mol. Psychiatr. 9, 609-*620*, 544.

Le Borgne, R., Alconada, A., Bauer, U., and Hoflack, B. (1998). The mammalian AP-3 adaptor-like complex mediates the intracellular transport of lysosomal membrane glycoproteins. J. Biol. Chem. *273*, 29451–29461.

Li, W., Rusiniak, M. E., Chintala, S., Gautam, R., Novak, E. K., and Swank, R. T. (2004). Murine Hermansky-Pudlak syndrome genes: regulators of lysosome-related organelles. Bioessays *26*, 616–628.

Martinez-Arca, S., *et al.* (2003). A dual mechanism controlling the localization and function of exocytic v-SNAREs. Proc. Natl. Acad. Sci. USA *100*, 9011–9016.

Matsuoka, K., Morimitsu, Y., Uchida, K., and Schekman, R. (1998). Coat assembly directs v-SNARE concentration into synthetic COPII vesicles. Mol. Cell *2*, 703–708.

Mirnics, K., Middleton, F. A., Marquez, A., Lewis, D. A., and Levitt, P. (2000). Molecular characterization of schizophrenia viewed by microarray analysis of gene expression in prefrontal cortex. Neuron *28*, 53–67.

Moriyama, K., and Bonifacino, J. S. (2002). Pallidin is a component of a multi-protein complex involved in the biogenesis of lysosome-related organelles. Traffic *3*, 666–677.

Mukaetova-Ladinska, E. B., Hurt, J., Honer, W. G., Harrington, C. R., and Wischik, C. M. (2002). Loss of synaptic but not cytoskeletal proteins in the cerebellum of chronic schizophrenics. Neurosci. Lett. *317*, 161–165.

Mullock, B. M., *et al.* (2000). Syntaxin 7 is localized to late endosome compartments, associates with Vamp 8, and is required for late endosome-lysosome fusion. Mol. Biol. Cell *11*, 3137–3153.

Nakatsu, F., *et al.* (2004). Defective function of GABA-containing synaptic vesicles in mice lacking the AP-3B clathrin adaptor. J. Cell Biol. *167*, 293–302.

Numakawa, T., *et al.* (2004). Evidence of novel neuronal functions of dysbindin, a susceptibility gene for schizophrenia. Hum. Mol. Genet. *13*, 2699–2708.

Owen, M. J., Craddock, N., and O'Donovan, M. C. (2005). Schizophrenia: genes at last? Trends Genet. *21*, 518–525.

Peden, A. A., Oorschot, V., Hesser, B. A., Austin, C. D., Scheller, R. H., and Klumperman, J. (2004). Localization of the AP-3 adaptor complex defines a novel endosomal exit site for lysosomal membrane proteins. J. Cell Biol. *164*, 1065–1076.

Peden, A. A., Park, G. Y., and Scheller, R. H. (2001). The Di-leucine motif of vesicle-associated membrane protein 4 is required for its localization and AP-1 binding. J. Biol. Chem. *276*, 49183–49187.

Peden, A. A., Rudge, R. E., Lui, W. W., and Robinson, M. S. (2002). Assembly and function of AP-3 complexes in cells expressing mutant subunits. J. Cell Biol. *156*, 327–336.

Prekeris, R., Klumperman, J., Chen, Y. A., and Scheller, R. H. (1998). Syntaxin 13 mediates cycling of plasma membrane proteins via tubulovesicular recycling endosomes. J. Cell Biol. *143*, 957–971.

Prekeris, R., Yang, B., Oorschot, V., Klumperman, J., and Scheller, R. H. (1999). Differential roles of syntaxin 7 and syntaxin 8 in endosomal trafficking. Mol. Biol. Cell *10*, 3891–3908.

Pryor, P. R., *et al.* (2004). Combinatorial SNARE complexes with VAMP7 or VAMP8 define different late endocytic fusion events. EMBO Rep. *5*, 590–595.

Robinson, M. S. (2004). Adaptable adaptors for coated vesicles. Trends Cell Biol. *14*, 167–174.

Ruder, C., Reimer, T., Delgado-Martinez, I., Hermosilla, R., Engelsberg, A., Nehring, R., Dorken, B., and Rehm, A. (2005). EBAG9 adds a new layer of control on large dense-core vesicle exocytosis via interaction with Snapin. Mol. Biol. Cell *16*, 1245–1257.

Salazar, G., Craige, B., Love, R., Kalman, D., and Faundez, V. (2005a). Vglut1 and ZnT3 co-targeting mechanisms regulate vesicular zinc stores in PC12 cells. J. Cell Sci. *118*, 1911–1921.

Salazar, G., Craige, B., Wainer, B. H., Guo, J., De Camilli, P., and Faundez, V. (2005b). Phosphatidylinositol-4-kinase type IIα is a component of adaptor protein-3-derived vesicles. Mol. Biol. Cell *16*, 3692–3704.

Salazar, G., and Gonzalez, A. (2002). Novel mechanism for regulation of epidermal growth factor receptor endocytosis revealed by protein kinase A inhibition. Mol. Biol. Cell *13*, 1677–1693.

Salazar, G., Love, R., Styers, M. L., Werner, E., Peden, A., Rodriguez, S., Gearing, M., Wainer, B. H., and Faundez, V. (2004a). AP-3-dependent mechanisms control the targeting of a chloride channel (ClC-3) in neuronal and non-neuronal cells. J. Biol. Chem. *279*, 25430–25439.

Salazar, G., Love, R., Werner, E., Doucette, M. M., Cheng, S., Levey, A., and Faundez, V. (2004b). The zinc transporter ZnT3 interacts with AP-3 and it is targeted to a distinct synaptic vesicle subpopulation. Mol. Biol. Cell *15*, 575–587.

Salem, N., Faundez, V., Horng, J. T., and Kelly, R. B. (1998). A v-SNARE participates in synaptic vesicle formation mediated by the AP3 adaptor complex. Nat. Neurosci. *1*, 551–556.

Seong, E., Wainer, B. H., Hughes, E. D., Saunders, T. L., Burmeister, M., and Faundez, V. (2005). Genetic analysis of the neuronal and ubiquitous AP-3 adaptor complexes reveals divergent functions in brain. Mol. Biol. Cell *16*, 128–140.

Shi, G., Faundez, V., Roos, J., Dell'Angelica, E. C., and Kelly, R. B. (1998). Neuroendocrine synaptic vesicles are formed in vitro by both clathrin-dependent and clathrin-independent pathways. J. Cell Biol. *143*, 947–955.

Springer, S., and Schekman, R. (1998). Nucleation of COPII vesicular coat complex by endoplasmic reticulum to Golgi vesicle SNAREs. Science *281*, 698–700.

Springer, S., Spang, A., and Schekman, R. (1999). A primer on vesicle budding. Cell *97*, 145–148.

Starcevic, M., and Dell'Angelica, E. C. (2004). Identification of snapin and three novel proteins (BLOS1, BLOS2, and BLOS3/reduced pigmentation) as subunits of biogenesis of lysosome-related organelles complex-1 (BLOC-1). J. Biol. Chem. *279*, 28393–28401.

Straub, R. E., Mayhew, M., Vakkalanka, R., Kolachana, B., Goldberg, T., Egan, M., and Weinberger, D. R. (2005). MUTED (6p24.3), a protein that binds to dysbindin (DTNBP1, 6p22.3), is strongly associated with schizophrenia and exhibits statistical epistasis with COMT. Neuropsychopharmacology *30*, S1–S270.

Styers, M. L., Salazar, G., Love, R., Peden, A. A., Kowalczyk, A. P., and Faundez, V. (2004). The endo-lysosomal sorting machinery interacts with the intermediate filament cytoskeleton. Mol. Biol. Cell *15*, 5369–5382.

Swedlow, J. R., Sedat, J. W., and Agard, D. A. (1997). Deconvolution in optical microscopy. In: Deconvolution of Images and Spectra, ed. P. A. Jansson, San Diego: Academic Press, 284–307.

Talbot, K., *et al.* (2004). Dysbindin-1 is reduced in intrinsic, glutamatergic terminals of the hippocampal formation in schizophrenia. J. Clin. Invest. *113*, 1353–1363.

Thiele, C., Hannah, M. J., Fahrenholz, F., and Huttner, W. B. (2000). Cholesterol binds to synaptophysin and is required for biogenesis of synaptic vesicles. Nat. Cell Biol. *2*, 42–49.

Tian, J. H., *et al.* (2005). The role of Snapin in neurosecretion: snapin knock-out mice exhibit impaired calcium-dependent exocytosis of large dense-core vesicles in chromaffin cells. J. Neurosci. *25*, 10546–10555.

Ward, D. M., Pevsner, J., Scullion, M. A., Vaughn, M., and Kaplan, J. (2000). Syntaxin 7 and VAMP-7 are soluble N-ethylmaleimide-sensitive factor attachment protein receptors required for late endosome-lysosome and homotypic lysosome fusion in alveolar macrophages. Mol. Biol. Cell *11*, 2327–2333.

Yang, W., Li, C., Ward, D. M., Kaplan, J., and Mansour, S. L. (2000). Defective organellar membrane protein trafficking in Ap3b1-deficient cells. J. Cell Sci. *113*, 4077–4086.